

Iterative Newton-Raphson-Based Impedance Method For Fault Distance Detection On Transmission Line

Ozuomba Simeon¹

Department of
Electrical/Electronic and
Computer Engineering,
University of Uyo, Akwa Ibom,
Nigeria

simeonoz@yahoo.com
simeonozuomba@uniuyo.edu.ng

Victor Akpaiya Udom²

Department of
Electrical/Electronic and
Computer Engineering,
University of Uyo, Akwa Ibom,
Nigeria

Jude Ibanga³

Department of
Electrical/Electronic and
Computer Engineering,
University of Uyo, Akwa Ibom,
Nigeria

Abstract— In this paper, an iterative Newton-Raphson-based impedance method for fault distance detection on a single three phase transmission line system with two generators is presented. The impedance method used the fault current and the fault voltage measured from both terminals of the transmission line based on the analytical expressions and the iterative Newton-Raphson flowchart for the fault distance estimation. A sample single three phase transmission line system was modeled in a MATLAB environment and simulation was conducted for different fault types and fault locations. Specifically, during the simulation, different types of faults were introduced at different locations along the transmission line and the measured phasor voltages and currents were used as input to the MATLAB program used to determine the fault location (distance) from the generators. The results showed that the impedance fault location method estimated fault location for each of the faults with a maximum fault location prediction error of 9.45%.

Keywords— *Impedance Method, Newton-Raphson Algorithm, Fault Distance, Fault Detection, Transmission Line System, Fault Current, Fault Voltage*

1. INTRODUCTION

Power transmission lines are subjected to different types of faults which have negative impact on the running and maintenance cost of the lines as well as negative impact on the clients of the power system output [1,2]. Accordingly, operators of power system networks seek for reliable methods to facilitate timely resolution of fault incidences.

In order to effectively address the fault situation, it is often important to detect and classify the fault and then, based on the fault category, the fault location determination procedure can be implemented [3,4,5,6]. Over the years, several methods have been developed for fault detection and classification while other methods have also been developed for fault location determination [7,8,9,10]. In this paper, the focus is on fault location determination on a three phase power transmission line. Among the different available method, an iterative Newton-Raphson-based impedance method for fault distance detection on transmission line is employed.

Whenever fault occurs on the transmission line (TL), phasor voltages and currents are generated and the voltages and currents waves propagate to each of the ends of the transmission line (TL) [11,12,13,14]. The impedance method uses the fault current and fault voltage measured from both terminal of the transmission line to determine the fault location [15,16]. In the double ended impedance based fault location method used in this paper, the synchronizing angle is required in the fault location model [17,18,19]. In the model, the initial value of the synchronizing angle is guesstimated. However, the iterative Newton-Raphson numerical iteration method is employed to determine the appropriate value of the synchronizing angle which will give a more accurate location value for the fault on the transmission line [20,21]. Sample case study transmission line was modelled using MATHLAB software and the simulation was conducted for different categories of faults on the transmission line and for different fault locations on the line. In each case, the iterative impedance method

presented in this paper was used to predict the fault location and the prediction performance of the method is assessed.

2. METHODOLOGY

The fault location analysis is conducted on a single three phase transmission line system with two generators, as shown in Figure 1. It is assumed that phasor voltage and current are available from the two ends of the single transmission line (TL). Specifically, whenever fault occurs on the TL, the phasor voltages and currents are measured from each of the ends of the TL. Then, the distance of the fault is calculated using the impedance method which is implemented using a program written in MATLAB. In this study, different types of faults are introduced at different locations along the TL and the measured phasor voltages and currents are used as input to the MATLAB program which uses the impedance method algorithm to determine the fault location (distance) from the generators.

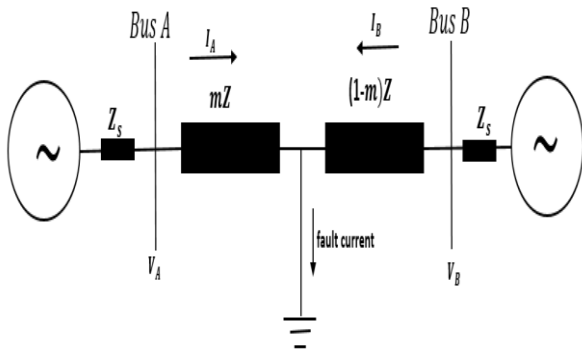


Figure 1: The line diagram of a faulted single three phase transmission line system with two generators
 (Source: [22]).

Consider a fault at a distance m from terminal A and the fault voltage, V_f is given as [22];

;

$$(V_f)_i = (V_A)_i - mZ_i \times (I_A)_i \quad (1)$$

$$(V_f)_i = (V_B)_i - (1 - m)Z_i \times (I_B)_i \quad (2)$$

Where $i = 0, 1, 2$ is the zero, positive and negative sequence; Z_s denotes the source impedance, V_A denotes the fault voltage at bus A, V_B denotes the fault voltage at bus B, I_A denotes the three phase fault current at bus A, I_B denotes the three phase fault current at bus B and Z denotes the line impedance where $Z = R + jX$. Equating the fault voltages in Equation (1) and Equation (2) gives;

$$(V_A)_i - (V_B)_i + Z_i(I_B)_i = mZ_i(I_A)_i + I_{Bi} \quad (3)$$

Since the data values from buses A and B are not synchronized, then synchronization is achieved by adding a synchronizing angle, δ . Then, the terminal voltages and the terminal currents of buses A and B becomes;

$$(V_A)_i = (V_A)_i < \alpha_i + \delta \quad (4)$$

$$(V_B)_i = (V_B)_i < \beta_i \quad (5)$$

$$(I_A)_i = (I_A)_i < \gamma_i + \delta \quad (6)$$

$$(I_B)_i = (I_B)_i < \theta_i \quad (7)$$

Where $\alpha, \beta, \gamma, \theta$ are the measured angles. Equation (3) in polar form becomes;

$$(V_A)_i e^{j\delta} - (V_B)_i + Z_i(I_B)_i = m \times Z_i \times (I_A)_i e^{j\delta} + I_{Bi} \quad (8)$$

Equation (4) in real and imaginary components becomes;

$$\begin{aligned} \text{Re}(V_A)_i \sin\delta + \text{Im}(V_A)_i \cos\delta - \text{Im}(V_B)_i + (C_4)_i = \\ m((C_1)_i \sin\delta + (C_2)_i \cos\delta + (C_4)_i) \end{aligned} \quad (9)$$

$$\begin{aligned} \text{Re}(V_A)_i \cos\delta - \text{Im}(V_A)_i \sin\delta - \text{Re}(V_B)_i + (C_3)_i = \\ m((C_1)_i \cos\delta - (C_2)_i \sin\delta + (C_3)_i) \end{aligned} \quad (10)$$

Where

$$(C_1)_i = R_i \times \text{Re}(I_A)_i - X_i \times \text{Im}(I_A)_i \quad (11)$$

$$(C_2)_i = R_i \times \text{Im}(I_A)_i + X_i \times \text{Re}(I_A)_i \quad (12)$$

$$(C_3)_i = R_i \times \text{Re}(I_B)_i - X_i \times \text{Im}(I_B)_i \quad (13)$$

$$(C_4)_i = R_i \times \text{Im}(I_B)_i + X_i \times \text{Re}(I_B)_i \quad (14)$$

The synchronizing angle, δ is determined as follows;

$$a_i \sin\delta + b_i \cos\delta + c_i = 0 \quad (15)$$

Where

$$\begin{aligned} a_i = -(C_3)_i \text{Re}(V_A)_i - (C_4)_i \text{Im}(V_A)_i - (C_1)_i \text{Re}(V_B)_i - \\ (C_2)_i \text{Im}(V_B)_i + (C_1)_i (C_3)_i + (C_2)_i (C_4)_i \end{aligned} \quad (16)$$

$$\begin{aligned} b_i = -(C_4)_i \text{Re}(V_A)_i - (C_3)_i \text{Im}(V_A)_i - (C_2)_i \text{Re}(V_B)_i + \\ (C_1)_i \text{Im}(V_B)_i + (C_2)_i (C_3)_i + (C_1)_i (C_4)_i \end{aligned} \quad (17)$$

$$\begin{aligned} c_i = -(C_2)_i \text{Re}(V_A)_i - (C_1)_i \text{Im}(V_A)_i - (C_3)_i \text{Re}(V_B)_i + \\ (C_4)_i \text{Im}(V_B)_i \end{aligned} \quad (18)$$

The iterative Newton-Raphson Method (NNM) is used to determine the synchronization angle. The equations used in the NNM for the determination of the synchronization angle are as follows;

$$\delta_{k+1} = \delta_k - \frac{F(\delta_k)}{F'(\delta_k)} \quad (19)$$

$$F(\delta_k) = b_i \cos\delta_k + a_i \sin\delta_k + c_i \quad (20)$$

$$F'(\delta_k) = a_i \cos\delta_k - b_i \sin\delta_k \quad (21)$$

In the Newton-Raphson method, an initial guess for δ is required. The iteration stops at the point where the difference between δ_{k+1} and δ_k is smaller than the tolerance value specified. After the synchronization angle, δ is determined, the fault location, m is computed from Equation (9) or Equation (10) as follows;

From Equation (9):

$$m = \frac{R_e(V_A)i \sin\delta + l m(V_A)i \cos\delta - l m(V_B)i + (C_4)i}{(C_1)i \sin\delta + (C_2)i \cos\delta + (C_4)i} \quad (22)$$

From Equation (10):

$$m = \frac{R_e(V_A)i \cos\delta - l m(V_A)i \sin\delta - R_e(V_B)i (C_3)i}{(C_1)i \cos\delta - (C_2)i \sin\delta + (C_3)i} \quad (23)$$

The flowchart for the iterative Newton-Raphson-based impedance model is presented in Figure 2. The model is simulated in MATLAB for different fault types and different fault locations on the case study transmission line.

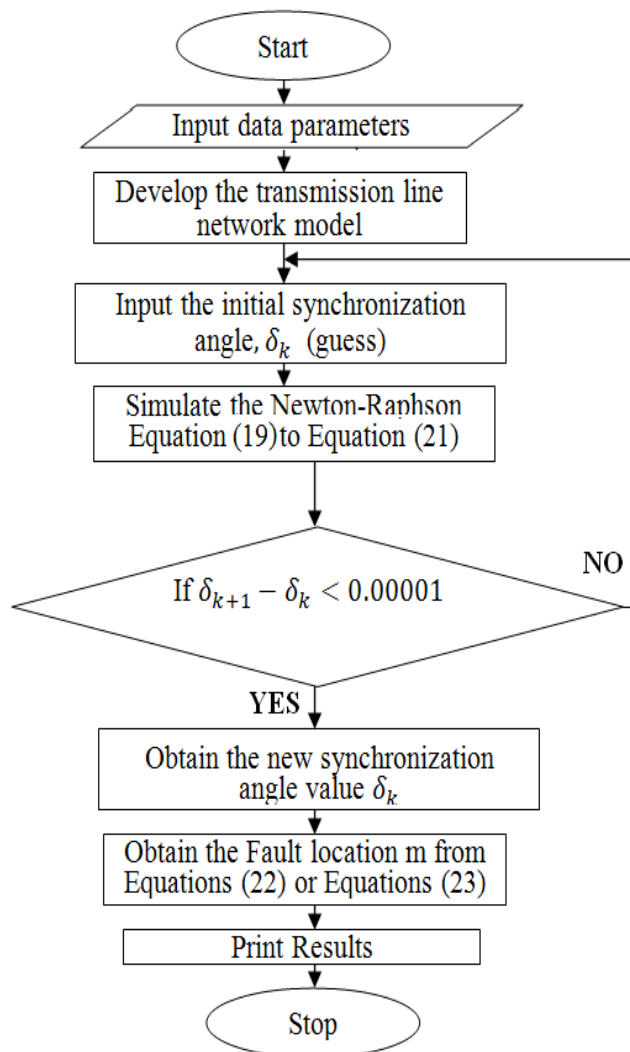


Figure 2: The flowchart for the iterative Newton-Raphson-based impedance method

The network for the implementation comprised of two (2) buses and two (2) transmission lines developed from the existing 330 kV transmission network in Nigeria.

The data used in this research were obtained from the operation records of Transmission Company of Nigeria (TCN) and also from some published related works. The system data along with the network modeled with short transmission line using Newton-Raphson method was simulated in MATLAB.

3.RESULTS AND DISCUSSION

The plot of the voltage against time for the three phases of the transmission line is shown in Figure 3. The total length of the line between bus A and bus B is 72 km. Fault occurred at 22.00 km away from bus A, the voltage waveform was stable at 330 kV or 1p.u until fault occurred at 0.015 sec then the voltage dipped to 25.10 kV or approximately 0.076 p.u.

The current waveform at bus A during a single phase to ground fault (A-G) is shown in Figure 4. The total length of the line between bus A and bus B was 72 km. Fault occurred at 22.00 km from bus A, the current waveform was stable until the fault occurred at 0.017 sec then the current increase to 900 A.

The plot of voltage against time for the three phases of the transmission line is shown in Figure 5. Fault occurred at 19.36 km away from bus A, voltage the waveform was stable at 330 kV or 1 p.u until fault occurred at 0.015 sec then the voltage dipped to 40.31 kV or approximately 0.122 p.u

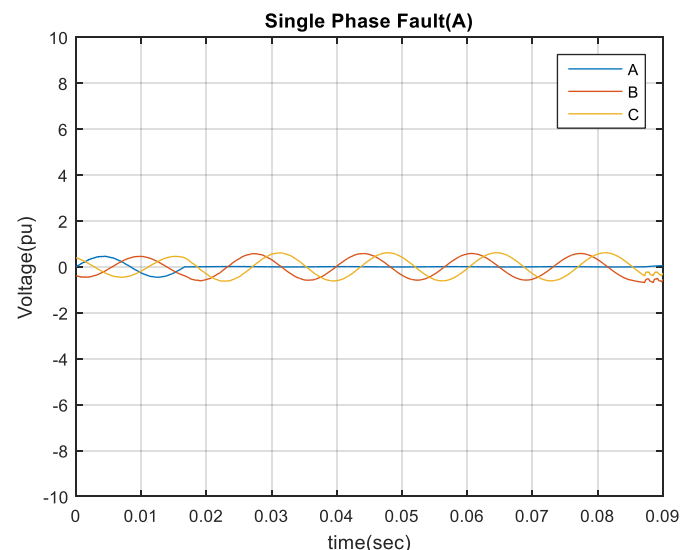


Figure 3: Voltage of single phase A-ground fault

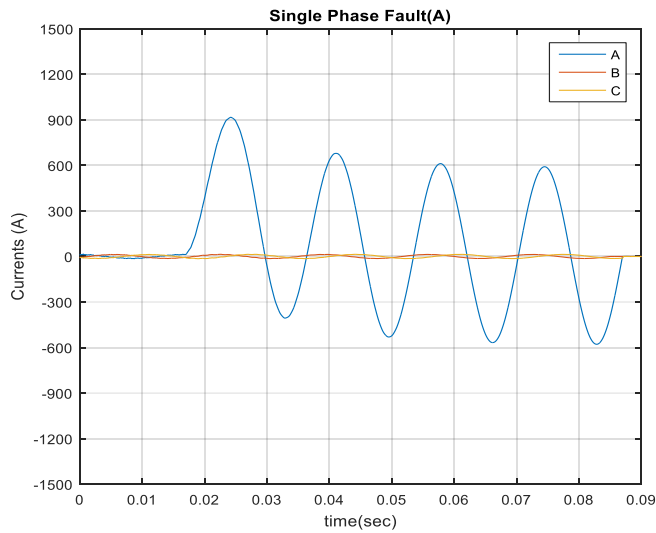


Figure 4: Current of single phase A-ground fault

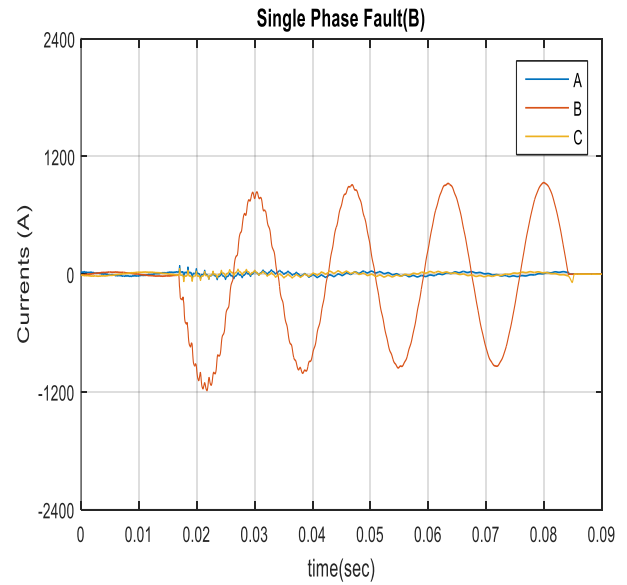


Figure 6: Current of single phase B-ground fault

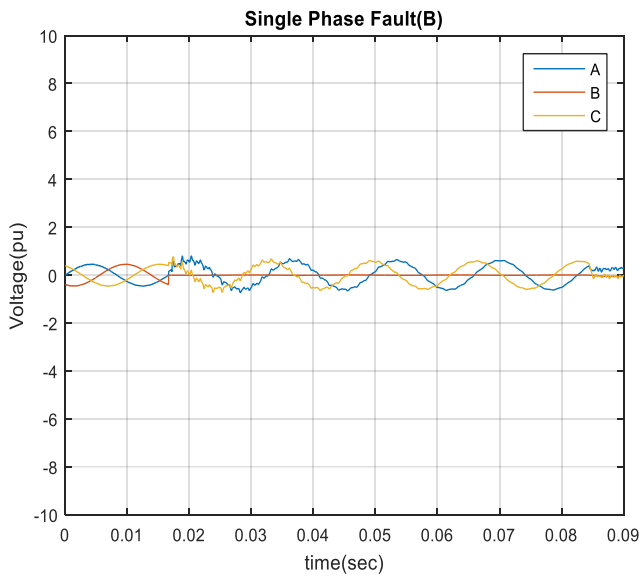


Figure 5: Voltage of single phase B-ground fault

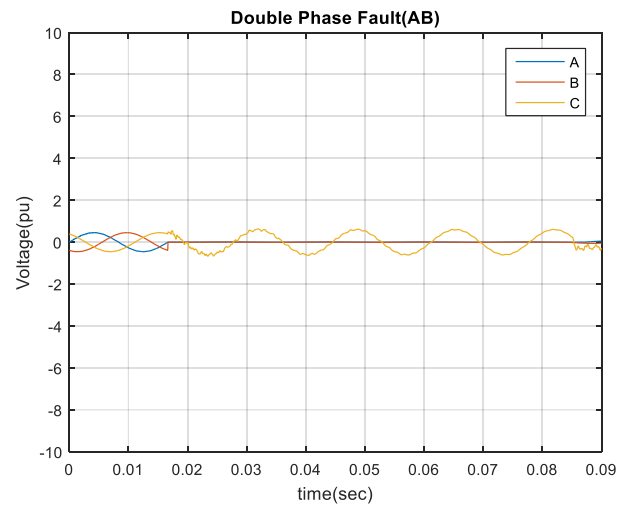


Figure 7: Voltage of double phase AB- ground fault

The current waveform at bus A during a single phase to ground fault (B-G) is shown in Figure 6. Fault occurred at 19.36 km from bus A, the current waveform was stable until the fault occurred at 0.02 sec then the current increased to 1100 A.

The plot of voltage against time of the three phases of the transmission line is shown in Figure 7. Fault occurred on phase A and B at 39.33 km away from bus A, the voltage waveform was stable at 330 kV or 1 p.u until fault occurred at 0.015 sec then the voltage dipped to 76.65 kV or approximately 0.23 p.u .

Figure 8 shows the current waveform at bus A during a double phase to ground fault (AB-G).

Fault occurred on phase A and B at 39.33 km from bus A, the current waveform was stable until the fault occurred at 0.017 sec then the current increased to 1100 A. The plot of voltage against time of the three phases of the transmission line is shown in Figure 9. Fault occurred on the three phases at 37.30 km away from bus A, the voltage waveform was stable at 330 kV or 1 p.u until fault occurred at 0.015 sec then the voltages for the three phases dipped to 90.12 kV or approximately 0.27 p.u.

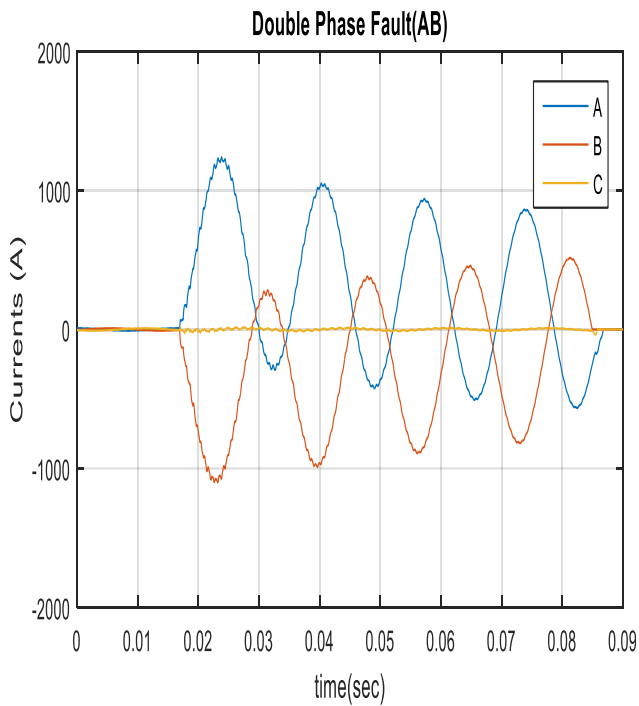


Figure 8: Current of double phase AB-ground fault

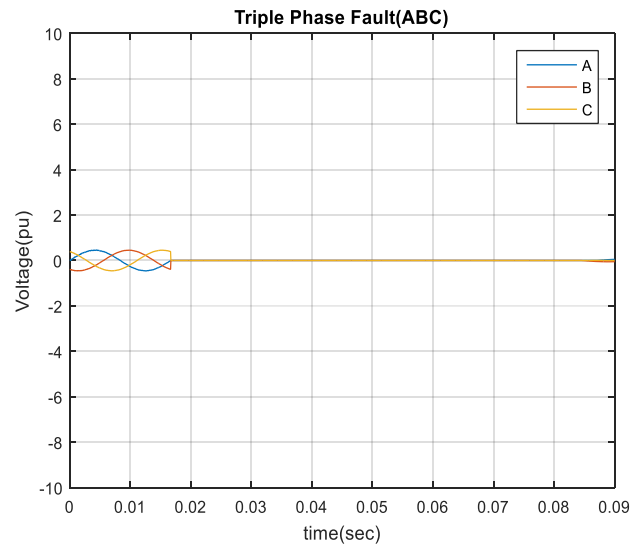


Figure 9: Voltage of triple phase ABC-ground fault

The simulation was conducted for different actual fault location .Table 1 shows the voltage and current values with actual fault distance. The impedance fault location method estimated fault location for each of the faults is noted as shown in Table 2. The maximum fault location prediction error noted was 9.45% .

Table 1: Voltage and current values with actual fault distance

S/N	Fault type	Voltage		Current		Actual distance (km)
		Magnitude (KV)	Phase (Deg)	Magnitude (A)	Phase (Deg)	
		1	A-G	25.10	300.21	
2	B-G	40.31	242.32	1114.32	710.41	19.36
3	AB-G	76.65	211.34	1102.41	700.65	39.33
4	ABC-G	90.12	186.22	1400.52	753.21	37.30

Table 2: Percentage error in fault distance using impedance and ANN methods

Fault type	Actual distance (km)	Impedance method (km)	% error with impedance method
A-G	22	19.92	-9.45
B-G	19.36	17.75	-8.32
AB-G	39.33	38.25	-2.75
ABC-G	37.3	36.5	-2.14

4. CONCLUSION

Fault location analysis is presented on a single three phase transmission line system with two generators. The

impedance method was used and the method uses fault current and fault voltage measured from both terminals of the transmission line. Specifically, the iterative Newton-

Raphson-based impedance method was used. The relevant analytical expressions and flowchart for the methodology are presented. A sample single three phase transmission line system was modeled in a MATLAB environment and simulation was conducted for different fault types and fault locations. The results showed that the method used in this paper can be used to estimate the fault location with percentage error less than 10%.

REFERENCES

1. Pinto Moreira de Souza, D., da Silva Christo, E., & Rocha Almeida, A. (2017). Location of faults in power transmission lines using the ARIMA method. *Energies*, 10(10), 1596.
2. Bhattacharya, B., & Sinha, A. (2017, November). Intelligent fault analysis in electrical power grids. In *2017 IEEE 29th International Conference on Tools with Artificial Intelligence (ICTAI)* (pp. 985-990). IEEE.
3. Thwe, E. P., & Oo, M. M. (2016). Fault Detection and Classification for Transmission Line Protection System Using Artificial Neural Network. *Journal of Electrical and Electronics Engineering*, 4(5), 89.
4. Sushama, M., Das, G. T. R., & Laxmi, A. J. (2009). Detection of high-impedance faults in transmission lines using wavelet transform. *ARPN Journal of Engineering and Applied Sciences*, 4(3), 6-12.
5. Jamil, M., Sharma, S. K., & Singh, R. (2015). Fault detection and classification in electrical power transmission system using artificial neural network. *SpringerPlus*, 4(1), 334.
6. Guillen, D., Paternina, M. R. A., Ortiz-Bejar, J., Tripathy, R. K., Zamora-Mendez, A., Tapia-Olvera, R., & Tellez, E. S. (2018). Fault detection and classification in transmission lines based on a PSD index. *IET Generation, Transmission & Distribution*, 12(18), 4070-4078.
7. Mouzakitis, A. (2013). Classification of fault diagnosis methods for control systems. *Measurement and Control*, 46(10), 303-308.
8. Katipamula, S., & Brambley, M. R. (2005). Methods for fault detection, diagnostics, and prognostics for building systems—a review, part I. *Hvac&R Research*, 11(1), 3-25.
9. Jian, X., Li, W., Guo, X., & Wang, R. (2019). Fault Diagnosis of Motor Bearings Based on a One-Dimensional Fusion Neural Network. *Sensors*, 19(1), 122.
10. Mujovic, S., Djukanovic, S., Radulovic, V., & Katic, V. A. (2016). Multi-parameter mathematical model for determination of PC cluster total harmonic distortion of input current. *COMPEL: The International Journal for Computation and Mathematics in Electrical and Electronic Engineering*, 35(1), 305-325.
11. Zhou, Y., Xu, G., & Chen, Y. (2012). Fault location in power electrical traction line system. *Energies*, 5(12), 5002-5018.
12. Bains, T. (2018). *New Algorithms for Locating Faults in Series Capacitive Compensated Transmission Lines* (Doctoral dissertation, The University of Western Ontario).
13. Lowe, B. S. (2015). *A new method of determining the transmission line parameters of an untransposed line using synchrophasor measurements* (Doctoral dissertation, Virginia Tech).
14. Yadav, A., & Thoke, A. S. (2011). Transmission line fault distance and direction estimation using artificial neural network. *International Journal of Engineering, Science and Technology*, 3(8), 110-121.
15. Personal, E., García, A., Parejo, A., Larios, D., Biscarri, F., & León, C. (2016). A comparison of impedance-based fault location methods for power underground distribution systems. *Energies*, 9(12), 1022.
16. Rahideh, A., Gitizadeh, M., & Mohammadi, S. (2013). A fault location technique for transmission lines using phasor measurements. *International Journal of Engineering and Advanced Technology (IJEAT)*, 3(1).
17. Roostae, S., Thomas, M. S., & Mehruz, S. (2017). Experimental studies on impedance based fault location for long transmission lines. *Protection and Control of Modern Power Systems*, 2(1), 16.
18. Personal, E., García, A., Parejo, A., Larios, D., Biscarri, F., & León, C. (2016). A comparison of impedance-based fault location methods for power underground distribution systems. *Energies*, 9(12), 1022.
19. Kang, N., Chen, J., & Liao, Y. (2015). A fault-location algorithm for series-compensated double-circuit transmission lines using the distributed parameter line model. *IEEE Transactions on Power Delivery*, 30(1), 360-367.
20. Thongkrajay, U., Poolsawat, N., Ratniyomchai, T., & Kulworawanichpong, T. (2006, March). Alternative Newton-Raphson power flow calculation in unbalanced three-phase power distribution systems. In *5th WSEAS International Conference on Applications of Electrical Engineering* (pp. 24-29).
21. Mohamed, D., Houari, S., & Tahar, B. (2012). Accurate fault location algorithm on power transmission lines with use of two-end unsynchronized measurements. *Serbian Journal of Electrical Engineering*, 9(2), 189-200.
22. Ghimire, S. (2014). Analysis of Fault location methods on transmission lines. Master's thesis at Tribhuvan University, Kathmandu, Nepal. Pp Available at <https://scholarworks.uno.edu/cgi/viewcontent.cgi?referer=https://scholar.google.com/&httpsredir=1&article=2842&context=td> Accessed on 5th February 2019.